Separation Science and Technology
Publication details, including instructions for authors and subscription information:
http://www.informaworld.com/smpp/title~content=t713708471

Use of Liquid Chromatography for Studying Reverse Osmosis and Ultrafiltration

Yutaka Taketani[a]; Takeshi Matsuura[a]; S. Sourirajan[a]
[a] DIVISION OF CHEMISTRY, NATIONAL RESEARCH COUNCIL OF CANADA, OTTAWA, CANADA

To cite this Article Taketani, Yutaka , Matsuura, Takeshi and Sourirajan, S.(1982) 'Use of Liquid Chromatography for Studying Reverse Osmosis and Ultrafiltration', Separation Science and Technology, 17: 6, 821 — 838
To link to this Article: DOI: 10.1080/01496398208058324
URL: http://dx.doi.org/10.1080/01496398208058324

SEPARATION SCIENCE AND TECHNOLOGY, 17(6), pp. 821–838, 1982

Use of Liquid Chromatography for Studying Reverse Osmosis and Ultrafiltration*

YUTAKA TAKETANI, TAKESHI MATSUURA,
and S. SOURIRAJAN

DIVISION OF CHEMISTRY
NATIONAL RESEARCH COUNCIL OF CANADA
OTTAWA, CANADA K1A OR9

Abstract

A method of observing the preferential adsorption of solute or solvent onto a polymer surface by liquid chromatography is illustrated, and the results are discussed in relation to the solute separation by reverse osmosis and membrane fouling. This method shows the existence of a preferentially adsorbed water layer at the polymer–solution interface, where its amount and thickness depend on the polymer material. The adsorption data of undissociated organic solutes indicate that cellulosic materials are intrinsically less susceptible to fouling by such solutes than synthetic polymer materials. It is also shown that the steric repulsion involved in the solute's distribution between the interfacial water phase and the bulk water phase is not sufficient to describe the solute transport through the membrane, and an additional steric effect associated with the frictional force working on the solute molecule in the membrane pore has to be considered.

INTRODUCTION

The interaction forces working in a membrane–solute–solvent system at the polymer–solution interfacial region and the structure of the membrane, which is often represented by the average pore size and pore size distribution on the membrane surface (*1*), are two governing factors of the solute and solvent transport in reverse osmosis and ultrafiltration membranes. Of these two factors, the interaction forces working at the polymer–solution interfacial region can be simulated by a liquid chromatography system in which the column is packed by the polymeric membrane material and the solute is injected into the solvent stream. The method of analyzing the data obtained by experiments in such a chromatography system was developed in our earlier work (*2*).

*NRC No. 20041.

The amount of interfacial water whose properties are different from that of ordinary bulk water, the thickness of the interfacial water layer, and the distribution coefficient of the solute between the interfacial water phase and the bulk water phase are three important interfacial properties which can be measured by high performance liquid chromatography (HPLC) methods as described above (*3*, *4*).

In this paper the methods developed in our earlier work (*2–4*) and new results are outlined. Further, the distribution coefficient of the solute is presented for many different solutes with respect to different polymeric membrane materials in different solvent systems. These experimental data are further discussed in terms of the appropriateness of the data to be used for the selection of membrane materials.

EXPERIMENTAL

HPLC Experiments

The liquid chromatograph model ALC 202 of Waters Associates fitted with a differential refractometer detector was used in this work. The structures of the repeating unit of polymers used in this study for packing the column are as listed in Table 1. The column details were the same as those reported earlier (*5*). Briefly, the particle size for the column was kept in the range 38–53 μm by sieving; the column material was packed dry in stainless steel tubes, 1/8 in. o.d., and 1/16 in. i.d., and the column length was 60 cm in most cases except CA-398 and CE columns whose lengths were 120 and 38 cm, respectively. Ten microliters of sample solution (solution concentration in the range of 1 ± 0.2%) was injected into the solvent stream (either water or methanol), and the retention volume of the chromatography peak for each solute was determined. In the case of heavy water and deuterated methanol, the solute concentration was 10%. All experiments were performed at laboratory temperature (23–25°C).

Reverse Osmosis Experiments

This work makes further use of reverse osmosis data already reported (*6–9*) for CA-398 316(10/30) membranes. The procedure of membrane making, the apparatus, and the experimental procedure have all been described in an earlier paper (*10*). The experimental procedures are described briefly as follows. Each membrane was subjected to an initial pure water pressure of 2068 kPa gauge (300 psig) for about 2 h prior to subsequent use in reverse osmosis experiments, all of which were carried out at 1724 kPa gauge (250 psig) and at laboratory temperature (23–25°C). The solute concentrations in the aqueous feed solutions were so low (0.001 to 0.006 *m*) that the osmotic pressures involved were negligible compared to the operating pressure. In each experiment, the fraction solute separation, defined as

$$f = \frac{\text{solute concentration in feed} - \text{solute concentration in product}}{\text{solute concentration in feed}}$$

membrane permeated product rate (PR), and pure water permeation rate (PWP) in kg/h for the effective area of membrane surface used (13.2 cm^2 in this work) were determined at the specified operating conditions. The concentrations of sodium chloride and other electrolyte solutes were determined by using a conductivity bridge and the concentrations of organic solutes were determined by a Beckman total carbon analyzer Model 915A.

THEORETICAL

The analysis of the HPLC data stems from the experimental observation that most inorganic electrolyte solutes and many organic polyfunctional solutes are eluted faster than heavy water whose retention time (or retention volume) can be regarded as identical to that of the solvent water (*2*). This phenomenon can be explained by the stronger adsorption of the solvent water than the solute onto the surface of polymer materials. The adsorbed water layer forms an interfacial water phase which has less dissolving ability for the solutes mentioned above than the ordinary bulk water. Based on the physicochemical concept described above, we have assumed the existence of two water phases, one which is the interfacial water phase and the other which is the bulk water phase. We further assume that these two phases constitute the stationary phase and the mobile phase described in HPLC theoretical developments. This is justified since the interfacial water necessarily has a significantly lower mobility than the bulk water phase. Then the retention volume V_R of a solute A can be written as

$$V_R = V_m + K'_A V_s \tag{1}$$

where V_m and V_s represent the volumes of the mobile and stationary phases and K'_A represents the equilibrium distribution coefficient for the solute (= concentration of the solute in the stationary phase/concentration of the solute in the mobile phase) (*2*). Since the experimental data for retention volume

TABLE 1

List of Polymers and Their Structures[a]

Polymer No.	Name of polymer	Symbol	Structure of repeating unit
1	Cellulose acetate	CA-398	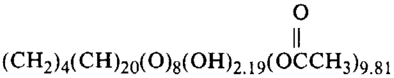 $(CH_2)_4(CH)_{20}(O)_8(OH)_{2.19}(O\overset{O}{\overset{\|}{C}}CH_3)_{9.81}$
2	Cellulose acetate	CA-376	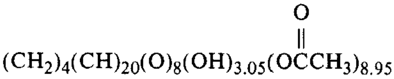 $(CH_2)_4(CH)_{20}(O)_8(OH)_{3.05}(O\overset{O}{\overset{\|}{C}}CH_3)_{8.95}$
3	Cellulose acetate	CA-383	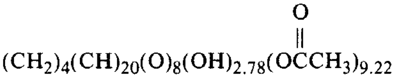 $(CH_2)_4(CH)_{20}(O)_8(OH)_{2.78}(O\overset{O}{\overset{\|}{C}}CH_3)_{9.22}$
4	Cellulose triacetate	CTA	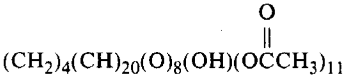 $(CH_2)_4(CH)_{20}(O)_8(OH)(O\overset{O}{\overset{\|}{C}}CH_3)_{11}$
5	Cellulose acetate propionate	CAP-151	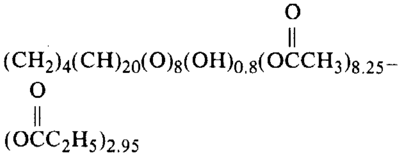 $(CH_2)_4(CH)_{20}(O)_8(OH)_{0.8}(O\overset{O}{\overset{\|}{C}}CH_3)_{8.25}-(\overset{O}{\overset{\|}{O}}CC_2H_5)_{2.95}$
6	Cellulose	CE	$(CH_2)_4(CH)_{20}(O)_8(OH)_{12}$
7	Aromatic copolyamide	PA	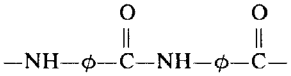 $-NH-\phi-\overset{O}{\overset{\|}{C}}-NH-\phi-\overset{O}{\overset{\|}{C}}-$
8	Aromatic copolyamidohydrazide	PPPH1115	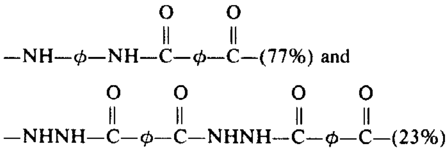 $-NH-\phi-NH-\overset{O}{\overset{\|}{C}}-\phi-\overset{O}{\overset{\|}{C}}-(77\%)$ and $-NHNH-\overset{O}{\overset{\|}{C}}-\phi-\overset{O}{\overset{\|}{C}}-NHNH-\overset{O}{\overset{\|}{C}}-\phi-\overset{O}{\overset{\|}{C}}-(23\%)$
9	Aromatic copolyhydrazide	PH	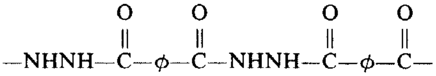 $-NHNH-\overset{O}{\overset{\|}{C}}-\phi-\overset{O}{\overset{\|}{C}}-NHNH-\overset{O}{\overset{\|}{C}}-\phi-\overset{O}{\overset{\|}{C}}-$
10	Aromatic copolyamidohydrazide	PPPH8273	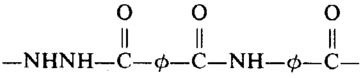 $-NHNH-\overset{O}{\overset{\|}{C}}-\phi-\overset{O}{\overset{\|}{C}}-NH-\phi-\overset{O}{\overset{\|}{C}}-$
11	Polypiperazineamide	Pip	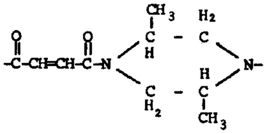
12	Polybenzimidazolone	PBIL	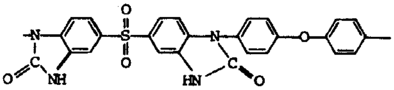

(continued)

TABLE 1 (continued)

Polymer No.	Name of polymer	Symbol	Structure of repeating unit
13	Aromatic polyimide	PI	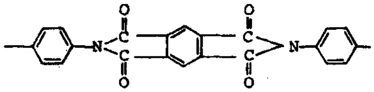 [b]
14	Nylon-6,6	Ny-6,6	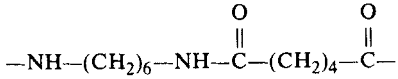 $-NH-(CH_2)_6-NH-\overset{O}{\overset{\|}{C}}-(CH_2)_4-\overset{O}{\overset{\|}{C}}-$
15	Polysulfone (Udel)	PS-U	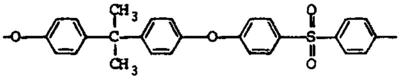
16	Polysulfone (Victrex)	PS-V	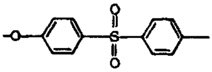
17	Polyvinyl formal	PVF	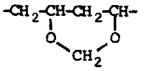
18	Polyvinyl butyral	PVB	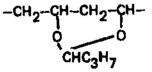
19	Polypropylene	PP	$-CH_2-CH(CH_3)-$
20	Polyethyl methacrylate	PEM	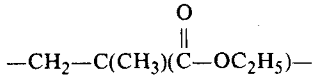 $-CH_2-C(CH_3)(\overset{O}{\overset{\|}{C}}-OC_2H_5)-$
21	Polydiallyl phthalate	PDP	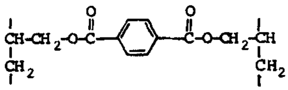
22	Polyether imine sulfone-urethane	PEIS-U	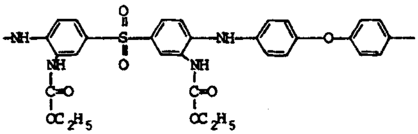

[a] ϕ = aromatic ring on which the position of substitution is *m*- or *p*-.

[b] Structure uncertain.

$[V'_R]$ include an amount of dead space V_d (caused by connecting tubes, fittings, refractometer cells, etc.), Eq. (1) can be written as

$$V'_R = V_R + V_d = V_m + V_d + K'_A V_s \qquad (2)$$

In order to calculate V_s and K'_A, the following K'_A values were assumed:

(1) $K'_A = 1$ for water (which is assumed to be the same as D_2O). This value is justified on the basis that the probability of a water molecule

to be in the mobile or the stationary phase is the same. When $K'_A = 1$, let $[V'_R] = [V'_R]_{\text{water}}$.

(2) The least retention volume among all solutes tested is considered equal to the retention volume of the mobile phase (plus that of the dead space). Let us designate such a retention volume as $[V'_R]_{\text{min}}$, then

$$[V'_R]_{\text{water}} = V_m + V_d + V_s \tag{3}$$

$$[V'_R]_{\text{min}} = V_m + V_d \tag{4}$$

Therefore,

$$V_s = [V'_R]_{\text{water}} - [V'_R]_{\text{min}} \tag{5}$$

Combining Eqs. (2), (4), and (5),

$$K'_A = \frac{[V'_R]_A - [V'_R]_{\text{min}}}{[V'_R]_{\text{water}} - [V'_R]_{\text{min}}} \tag{6}$$

Equations (5) and (6) enable the calculation of V_s and K'_A by measuring the retention volumes as required in the equations.

It has to be noted that a significant error is contained in the value of K'_A calculation by Eq. (6), since the denominator of Eq. (6) involves a small difference in two large quantities (*11*). Despite the error, K'_A values thus obtained are meaningful in many physicochemical aspects and, therefore, serve as a practical measure for representing solute–polymer interaction.

In the methanol solvent system the analytical procedure is exactly the same as in the water solvent system except that deuterated methanol was used instead of heavy water.

RESULTS AND DISCUSSION

Volume of the Interfacial Water and Thickness of the Interfacial Water Layer

When V_s is divided by the weight of the polymer packing material in the chromatography column designated as m, the resulting quantity V_s/m indicates the specific volume of interfacial water per unit mass of the polymer material. A large value of V_s/m indicates that the polymer material is rich in interfacial water, which is a desirable property for a polymeric membrane material for the separation of electrolyte solutes since interfacial water has a reduced dissolving power for such solutes compared to ordinary bulk water.

The quantity V_s/m was measured for 22 polymers and the result is listed in Table 2 (4). V_s/m vaues were further split into the contributions from the structural components. For this purpose, an additivity principle was applied to the different structural components of the polymer repeating unit, as expressed by

$$\Sigma\zeta_i = (V_s/m)(\Sigma(\mathrm{F.W.})_i) \tag{7}$$

where ζ_i and $(\mathrm{F.W.})_i$ indicate the contribution of *i*th structural component to interfacial water volume and the formula weight of *i*th structural component, respectively, and the summation extends over the repeating unit of the polymer structure. By multiplying the formula weight of the polymer repeating unit, $\Sigma(\mathrm{F.W.})_i$, on the right side of Eq. (7), the interfacial volume is expressed per unit mole of the polymer repeating unit. For example, Eq. (7) can be applied to PA polymer material (polymer number 7) as

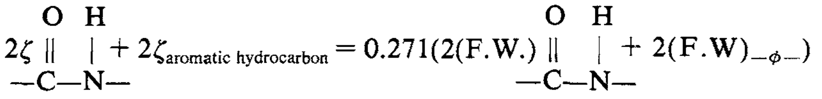

$$2\zeta\ \underset{\text{—C—N—}}{\overset{\text{O H}}{\text{‖ |}}} + 2\zeta_{\text{aromatic hydrocarbon}} = 0.271\left(2(\mathrm{F.W.})\ \underset{\text{—C—N—}}{\overset{\text{O H}}{\text{‖ |}}} + 2(\mathrm{F.W})_{-\phi-}\right) \tag{8}$$

Equation (7) was applied to 21 polymer materials listed in Table 1 (PI polymer was excluded due to the uncertainty of the polymer structure). Thus we were able to obtain 21 linear equations analogous to Eq. (8) and they could be solved simultaneously with respect to nine unknown ζ_i values corresponding to structural components listed in Table 3 by linear regression analysis. The result is also listed in Table 3. The quantity ζ_i thus obtained expresses interfacial water volume attached to a unit mole of structural component.

When the interfacial volume is further converted to the molar amount of interfacial water, the resulting quantities (also listed in the last column of Table 3) indicate the number of moles of interfacial water per unit mole of the structural component, which are equivalent to the number of interfacial water molecules adsorbed onto one structural component. The values thus generated reveal several interesting features of the interfacial water adsorbed from the liquid phase water.

(1) The number of interfacial water molecules associated with each structural component is less than three.

(2) Structural components such as aromatic hydrocarbon, —OH, $\overset{\text{O}}{\overset{\|}{\text{—C—O—}}}$, —O—, $\overset{\text{O H}}{\overset{\text{‖ |}}{\text{—C—N—}}}$, and $\overset{\text{O}}{\overset{\|}{\text{>N—C—}}}$ exhibit positive con-

TABLE 2

Data for V_s/m for Different Polymers

Polymer	$(V_s/m) \times 10^3$ m^3/kg	Polymer	$(V_s/m) \times 10^3$ m^3/kg
CA-398	0.233	PBIL	0.085
CA-376	0.380	PI	0.297
CA-383	0.502	NY-6,6	0.464
CTA	0.149	PS-U	0.140
CAP-151	0.290	PS-V	0.080
CE	0.236	PVF	0.343
PA	0.271	PVB	0.135
PPPH 1115	0.543	PP	0.180
PH	0.385	PEM	0.020
PPPH 8273	0.539	PDP	0.148
Pip	0.499	PEIS-U	0.152

TABLE 3

Structural Contribution to V_s/m

Structural component	Contribution to V_s/m	
	$\zeta_i \times 10^6$, m^3 / mol. component	number of H_2O / unit component
Aliphatic hydrocarbon	−2.03	−0.11
Aromatic hydrocarbon	6.38	0.35
—OH	3.00	0.17
$-\overset{\overset{\displaystyle O}{\|}}{C}-O-$	23.27	1.29
—O—	25.70	1.43
—CONH—	38.04	2.11
>NCO—	49.73	2.76
>NH	−40.20	−2.23
$-SO_2-$	−14.27	−0.79

tributions, while aliphatic hydrocarbon, >NH, and $-\overset{\overset{\displaystyle O}{\|}}{\underset{\underset{\displaystyle O}{\|}}{S}}-$ groups exhibit negative contributions, indicating that the presence of a structural component from the latter group diminshes the amount of interfacial water.

(3) Nitrogen-containing functional groups such as 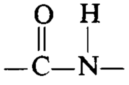 $-\overset{O}{\overset{\|}{C}}-\overset{H}{\overset{|}{N}}-$ and 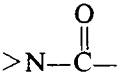 $>N-\overset{O}{\overset{\|}{C}}-$ are preferable for the formation of interfacial water than functional groups which contain oxygen only. The contribution from —OH group is surprisingly small.

(4) The contribution from amide groups is strongly diminished by the presence of a >NH group, particularly in the case of PBIL and PEIS-U polymers.

From the effect of the structural component on the contribution to V_s/m, it can be concluded that aromatic hydrocarbon is preferable to aliphatic hydrocarbon and that the 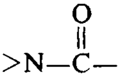 $>N-\overset{O}{\overset{\|}{C}}-$ group is the best among all of the polar functional groups considered.

Since the specific volume of interfacial water, V_s/m was obtained as listed in Table 2, the thickness of interfacial water, designated as t, can be calculated if the specific area of the polymer material is known. Therefore, the specific surface areas of several cellulose acetate samples were measured by monolayer adsorption of *p*-nitrophenol in aqueous solutions at laboratory temperature (23–25°C) using the method of Giles et al. (*12–14*). The adsorption isotherm of *p*-nitrophenol obtained for CA-398 material is as illustrated in Fig. 1. The specific surface area, m^2/kg of polymer, of the polymer sample was calculated from the plateau corresponding to the monolayer formation on the basis that the area occupied by each *p*-nitrophenol molecule is $25\,\text{Å}^2$ and the result is listed in Table 4. Dividing V_s/m, m^3/kg-polymer, reported in Table 2 by the specific surface area shown in Table 4, the thickness of the interfacial water layer, t, was obtained and the result is also listed in Table 4. This result indicates that t ranges from 0.68 to 2.12 nm with the particular polymers investigated and depends on the polymer material.

Distribution Coefficients K'_A

Figure 2 shows K'_A values for different alcohols with respect to CA-398 polymer material. It is obvious from the figure that K'_A of normal alcohols increases with the increase in the number of carbon atoms, while the increase in the degree of branching in the hydrocarbon substituent group decreases K'_A. This result indicates that the increase in hydrophobicity of the alcoholic molecule with an increase in the length of the hydrocarbon chain leads to a stronger adsorption of the solute molecule onto the polymer surface, while

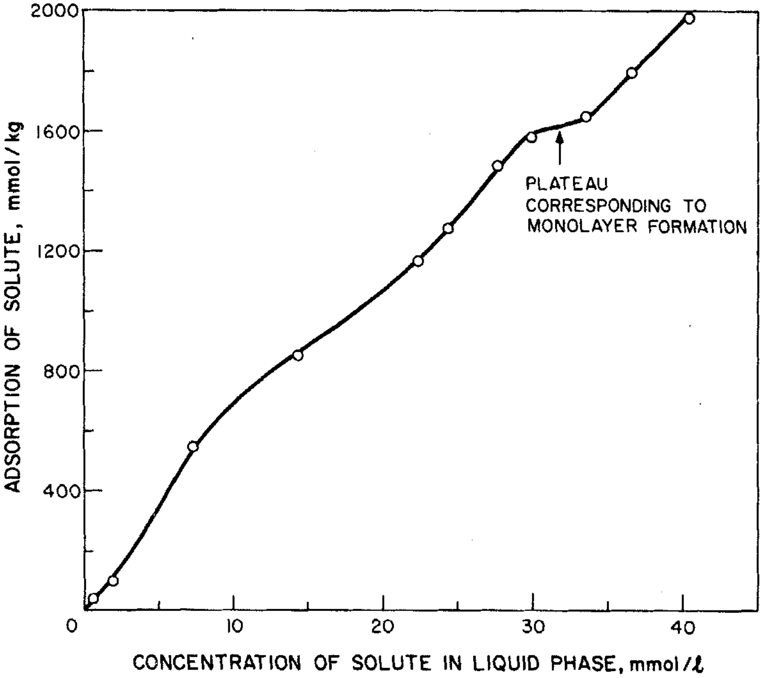

FIG. 1. Adsorption isotherm of *p*-nitrophenol from an aqueous solution onto cellulose acetate (CA-398) polymer material at laboratory temperature.

the increase in bulkiness of the alcoholic molecule by branching of the hydrocarbon chain results in steric repulsion from the polymer surface.

Figure 3 illustrates K'_A values for different inorganic and organic solutes with respect to CA-398 polymer material. Several important features of solute adsorption onto this particular polymer material are shown in the this figure.

TABLE 4

Data for the Specific Surface Area and Thickness of Interfacial Water

	Polymer		
	CA-398	CA-383	CTA
Specific surface area × 10^{-3}, m^2/kg	237.8	244.3	214.8
Thickness of interfacial water layer, nm	0.95	2.12	0.68

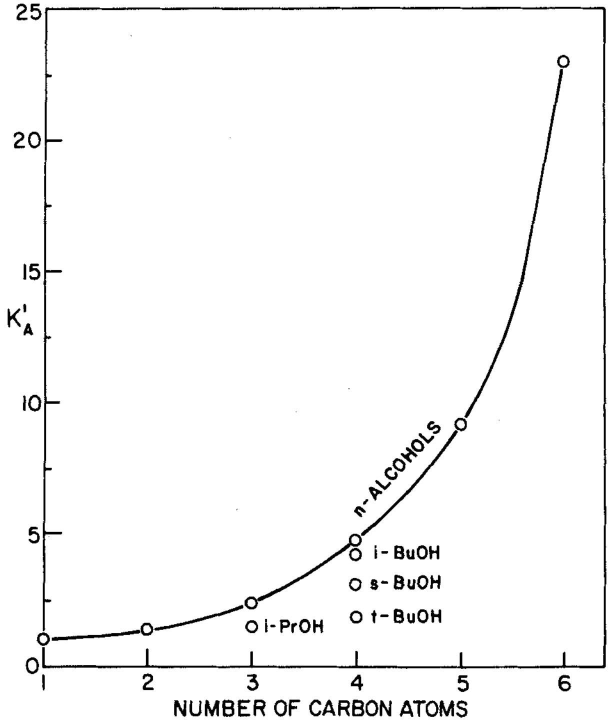

FIG. 2. K'_A of different alcohols with respect to cellulose acetate (CA-398) polymer material at laboratory temperature.

(1) Inorganic electrolyte solutes are generally more strongly rejected from the polymer–solution interface than organic solutes.

(2) Among inorganic solutes, those which are comprised of divalent ions (example, Na_2SO_4) are more strongly rejected than those which are comprised of monovalent ions (example, NaCl). Inorganic solutes with little dissociation (example, H_3BO_3) are least rejected from the polymer–solution interface. H_3BO_3 is even slightly enriched in the interfacial water phase.

(3) Though undissociated organic solutes are usually less rejected than inorganic electrolytes, solutes such as carbohydrates (example, glucose) are rejected as strongly as electrolyte solutes. Organic compounds with more than one polar functional group (example, ethylene glycol) are also rejected from the polymer–solution interface. This rejection is caused by the negative van der Waals force which is the result of the stronger attracive force working between the solute

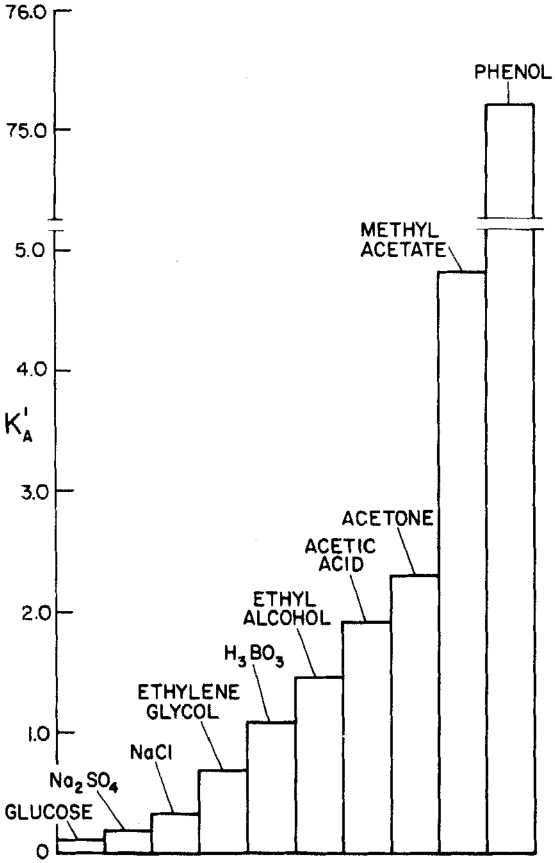

FIG. 3. K'_A of different inorganic and organic solutes with respect to cellulose acetate (CA-398) polymer material at laboratory temperature.

and the solvent water as compared to that working between the solute and the surface of the polymer material.

(4) Undissociated polar organic solutes with one polar functional group such as ethanol, acetic acid (regarded as undissociated), acetone, and methyl acetate exhibit K'_A values of greater than unity, indicating the enrichment of these solutes in the interfacial water phase, which is equivalent to the preferential adsorption of these solutes onto the surface of the polymer material.

(5) Solutes with aromatic rings (example, phenol) are adsorbed onto the polymer surface most strongly.

Thus K'_A values determined by HPLC methods express precisely the relative strength of the interaction forces (either attractive or repulsive) working between the solute and the polymer surface.

The effect of polymer material on K'_A is illustrated in Fig. 4, where K'_A values of normal alcohols (from C_3 to C_6) in the water solvent system are shown with respect to CE, CA-398, PS-V, and PPPH8273 polymers. In Fig. 4, K'_A values in the methanol solvent system are also shown (filled circle) with respect to CA-398 polymeric material. From Fig. 4 it is very obvious that the decreasing order of K'_A values in the water solvent system was observed as PPPH 8273 > PS-V > CA-398 > CE for all normal alcoholic solutes used. While K'_A values with respect to PPPH 8273, PS-V, and CA-

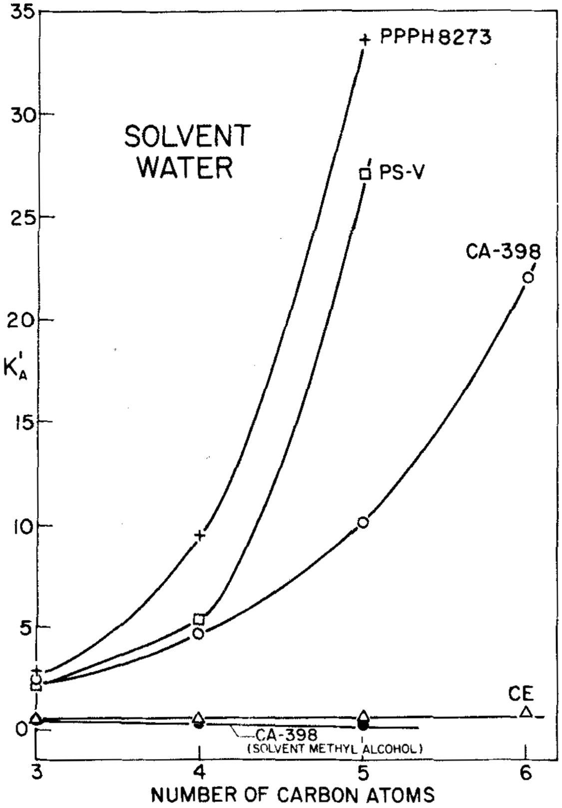

FIG. 4. K'_A of normal alcohols with respect to cellulose, cellulose acetate (CA-398), polysulfone (Victrex), and polyamidohydrazide (PPPH8273) polymer materials in water and methanol solvent systems at laboratory temperature.

398 polymers increase with an increase in the number of carbon atoms, K'_A values with respect to CE polymeric material are almost unchanged, indicating that the attractive force of solvent water and CE polymer material toward alcoholic solutes are almost unchanged with the number of carbon atoms. This is reasonable when the high hydrophilicity of cellulose polymer material is considered. In any case, CE polymer material exhibits the smallest, while PPPH 8273 polymer material exhibits the largest adsorption capacity to normal alcoholic solutes. This result may also be generalized to include the case of other undissociated organic solutes. Since membranes with a high adsorption capacity for undissociated organic solutes are intrinsically more susceptible to "fouling" by the latter solutes, the decreasing order in K'_A values mentioned above corresponds directly to the decreasing order of the susceptibility of polymeric membrane materials to "fouling."

The K'_A values for methanol solvent systems are less than unity, indicating that alcoholic solute molecules are more strongly attracted toward the methanol solvent. It is also interesting to note that K'_A values decrease with the increase in the number of carbon atoms in alcoholic solutes, which indicates that the increase in the hydrophobic nature of the solute enhances the attraction to the methanol solvent rather than to the cellulose acetate polymer material. Further, the lower K'_A values in methanol solvent than those observed in the water solvent system means that membranes made of CA-398 material can be cleaned by switching the solvent from water to methanol when the membrane surface is contaminated by undissociated organic compounds in the water solvent system. Thus K'_A alone offers a means of choosing membrane materials which are less susceptible to "fouling" by undissociated organic solutes as well as a means of finding an effective cleaning device when the membrane surface is contaminated.

Another example of the change in adsorption capacity by different polymeric materials is demonstrated by K'_A values for polyethylene glycols of different molecular weight with respect to CA-398 and PS-V polymer materials. As illustrated in Fig. 5, K'_A values for all polyethylene glycol solutes are less than unity with respect to CA-398 material and decrease with an increase in molecular weight, while K'_A values with respect to PS-V material start from 0.64 at a molecular weight of 200, gradually increase up to 2.41 at a molecular weight of 400, then gradually decrease to 1.22 at a molecular weight of 1000, and increase again to 38.06 at a molecular weight of 4000. This complicated picture of polyethylene glycol adsorption onto PS-V polymer material is probably the result of the superimposed effects of increasing hydrophobic affinity and increasing steric repulsion working between the polymer surface and the polyethylene glycol solutes with the

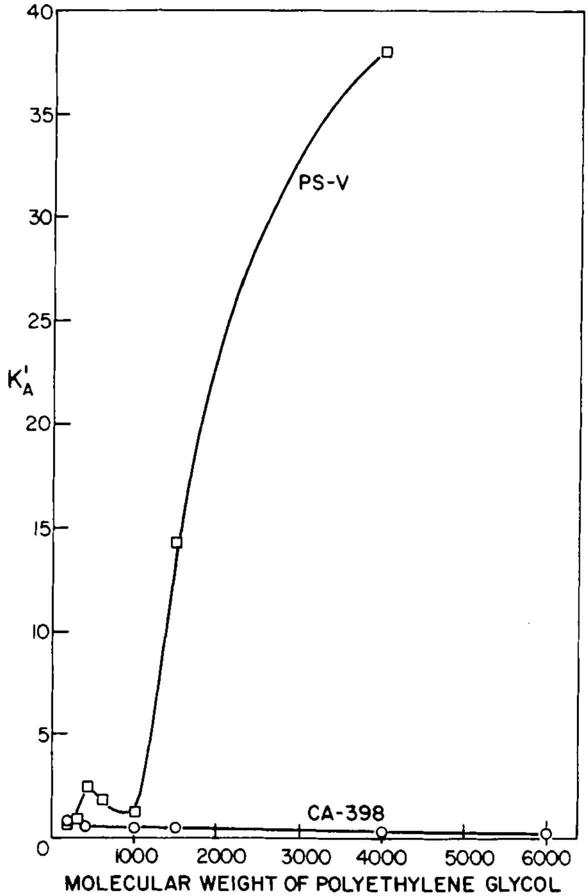

FIG. 5. K'_A of polyethylene glycols with respect to cellulose acetate (CA-398) (○) and polysulfone (Victrex) (□) polymer materials at laboratory temperature.

increase in molecular weight. In any case, it can be concluded from Fig. 5 that polyethylene glycol solute of molecular weight above 300 are preferentially adsorbed onto the PS-V polymer surface in contrast to the CA-398 polymer surface where water is preferentially adsorbed. The greater affinity force working between polyethylene glycol solutes and PS-V material compared to that working between these solutes and CA-398 material can probably be generalized to other high molecular weight solutes. Since the interaction between membrane material and macromolecular solutes is one of the factors governing the performance of ultrafiltration membranes, the determination of such an interaction force by HPLC methods offers a means of investigating the ultrafiltration process, particularly in terms of the formation of gel layer and the blocking of membrane pores.

Relationship between K'_A and Solute Separation by Reverse Osmosis

In Fig. 6, separations of different solutes by a particular membrane made of CA-398 material are plotted against K'_A values with respect to CA-398 polymeric material. Figure 6 indicates that with solutes whose K'_A values are below 0.33, separations are greater than 90% while solute separations are less than 10% with solutes whose K'_A values are above 40. Thus, K'_A values alone correlate satisfactorily to solute separations in these ranges of K'_A. However, in the intermediate range of K'_A, the correlation of K'_A with solute separation is not very satisfactory. For example, desipte the narrow range of the change in K'_A values with respect to ethyl alcohol, isopropyl alcohol and *t*-butyl alcohol, from 1.47 to 1.90, the solute separation changes from 23 to 79%. The Stokes' law radius of the latter three solutes are 0.205, 0.226, and 0.335 nm, respectively, indicating that K'_A values alone do not

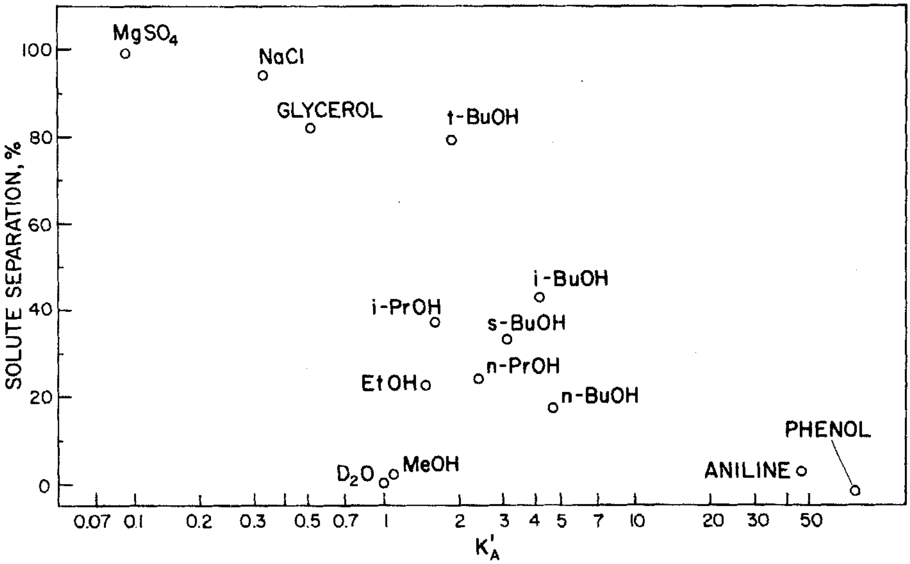

FIG. 6. K'_A versus solute separation. Reverse osmosis experiment. Membrane, cellulose acetate (CA-398) 316 (10/30). Operating pressure, 1724 kPa gauge (= 250 psig). Solute concentration <0.006 *m*. Feed flow rate, 400 × 10^{-6} m^3/min.

determine the solute separation but the bulkiness of the solute molecule is also an effect. Since it was already shown that the effect of steric repulsion working between the membrane material and the solute molecule on the value of K'_A was taken into consideration, the above result clearly indicates that there is an additional effect of stericity of the solute molecule on solute transport through membrane pores which was not counted in the steric effect on K'_A. These two steric effects, one on the concentration equilibrium at the polymer–solution interface and the other on the frictional force working on the solute molecule while it is moving in the membrane pore, were treated more rigorously in our earlier work on the surface force–pore flow model (*15*, *16*).

CONCLUSION

The amount of interfacial water per unit mole of polymer repeating unit was split into the contribution from structural components and it was found that the combination of aromatic hydrocarbon and 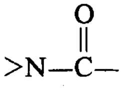 $>\mathrm{N}{-}\overset{\overset{\displaystyle \mathrm{O}}{\|}}{\mathrm{C}}{-}$ functional group is a preferable structure to contain a large amount of interfacial water. The interfacial water phase has a lower dissolving power to electrolyte and polyfunctional organic solutes and therefore a large amount of interfacial water is desirable for reverse osmosis membrane materials for separation of such solutes.

It was also shown that the polymer materials with lower K'_A values for undissociated organic solutes have to be chosen to diminish the "fouling" of the membrane by such solutes.

Despite the contribution of the steric effect on the distribution coefficient of solute between interfacial water phase and bulk water phase, K'_A, it is not sufficient to explain a large steric hindrance during the solute movement in the membrane pore. An additional steric effect associated with the friction working on the solute molecule in the membrane pore has to be considered.

Thus the results from HPLC experiment are useful for the further elucidation of membrane transport phenomena.

REFERENCES

1. S. Sourirajan, *Reverse Osmosis*, Academic, New York, 1970, Chap. 3.

2. T. Matsuura and S. Sourirajan, *J. Colloid Interface Sci., 66*, 589 (1978).

3. T. Matsuura, Y. Taketani, and S. Sourirajan, *J. Membr. Sci.*, In Press.

4. T. Matsuura, Y. Taketani, and S. Sourirajan, *Desalination, 38*, 319 (1981).

5. T. Matsuura, P. Blais, and S. Sourirajan, *J. Appl. Polym. Sci., 20*, 1515 (1976).

6. T. Matsuura and S. Sourirajan, *Ibid.*, *15*, 2905 (1971).
7. T. Matsuura and S. Sourirajan, *Ibid.*, *17*, 1043 (1973).
8. R. Rangarajan, T. Matsuura, E. C. Goodhue, and S. Sourirajan, *Ind. Eng. Chem., Process Des. Dev.*, *15*, 529 (1976).
9. T. Matsuura and S. Sourirajan, *J. Appl. Polym. Sci.*, *16*, 1663 (1972).
10. L. Pageau and S. Sourirajan, *Ibid.*, *16*, 3185 (1972).
11. Y. Taketani, T. Matsuura, and S. Sourirajan, *J. Electrochem. Soc.*, In Press.
12. C. H. Giles, T. H. MacEwan, S. N. Nakhwa, and D. Smith, *J. Chem. Soc.*, p. 3973 (1960).
13. C. H. Giles and S. N. Nakhwa, *J. Appl. Chem.*, *12*, 266 (1962).
14. H. S. Blair and M. J. McElroy, *J. Appl. Polym. Sci.*, *19*, 3161 (1975).
15. T. Matsuura and S. Sourirajan, *Ind. Eng. Chem., Process Des. Dev.*, *20*, 273 (1981).
16. T. Matsuura, Y. Taketani, and S. Sourirajan, in *Synthetic Membranes*, Vol. II (A. F. Turbak, ed.), ACS Symposium Series 154, 1981, p. 315.

Received by editor September 1, 1981